HHS Public Access

Author manuscript

J Am Coll Cardiol. Author manuscript; available in PMC 2016 August 11.

Published in final edited form as:

J Am Coll Cardiol. 2015 August 11; 66(6): 599–611. doi:10.1016/j.jacc.2015.05.068.

Exosomes from cardiac stem cells amplify their own bioactivity by converting fibroblasts to therapeutic cells

Eleni Tseliou, MD[*], **Joseph Fouad**[†], **Heidi Reich, MD**[*], **Leandro Slipczuk, MD**[*], **Geoffrey de Couto, PhD**[*], **Mark Aminzadeh, MD**[*], **Ryan Middleton, MS**[*], **Jackelyn Valle, BS**[*], **Liu Weixin, MS**[*], and **Eduardo Marbán, MD, PhD**[*]

[*]Cedars-Sinai Heart Institute, Los Angeles, California

[†]Harvard College, Boston, Massachusetts

Abstract

BACKGROUND—Cardiosphere-derived cells (CDCs) mediate therapeutic regeneration in patients after myocardial infarction and are undergoing further clinical testing for cardiomyopathy. The beneficial effects of CDCs are mediated by the secretion of exosomes and possibly other extracellular membrane vesicles (EMV).

OBJECTIVES—We investigated the effect of cardiosphere-derived EMVs (CSp-EMV) on fibroblasts in vitro and tested whether priming with CSp-EMV could confer salutary properties on fibroblasts in vivo.

METHODS—CSp-EMVs were isolated from serum-free media conditioned for 3 days by cardiospheres. Dermal fibroblasts were primed with CSp-EMV for 24 h followed by exosomal micro-ribonucleic acid (miRNA) profiling. In vivo, we injected CSp-EMV-primed or -unprimed dermal fibroblasts (or CSp-EMV) in a chronic rat model of myocardial infarction and defined the functional and structural consequences.

RESULTS—CSp-EMV amplified their own biological signals: exposure of “inert” fibroblasts to CSp-EMV rendered the fibroblasts therapeutic. Intramyocardially-injected CSp-EMV-primed (but not unprimed) fibroblasts increased global pump function and vessel density while reducing scar mass. CSp-EMV priming caused fibroblasts to secrete much higher levels of stromal-cell derived factor 1 and vascular endothelial growth factor, and dramatically changed the microRNA profile of fibroblast-secreted EMVs in vitro. The priming was followed by significant angiogenic and cardioprotective effects.

Corresponding Author: Eduardo Marbán MD, PhD, Cedars-Sinai Heart Institute, 8700 Beverly Blvd, Los Angeles, CA 90048, Fax: 310-4237637, Eduardo.Marban@csmc.edu.

DISCLOSURES

The authors had full access to and take full responsibility for the integrity of the data. All authors have read and agree to the manuscript as written. EM owns equity in Capricor and serves as an unpaid advisor to Capricor. Other authors have no relationships with industry.

NOTIFICATION Herman K. Gold Young Investigator's Award in Molecular and Cellular Cardiology at ACC.2015

CONCLUSIONS—CSp-EMVs alter fibroblast phenotype and secretome in a salutary positive-feedback loop. The phenotypic conversion of inert cells to therapeutically-active cells reveals a novel mechanism for amplification of exosome bioactivity.

Keywords

cardiac repair; conversion; exosome; growth factor

INTRODUCTION

Paracrine signaling mediates the therapeutic benefits of cardiospheres (1) and their progeny (2) (cardiosphere-derived cells [CDC]). Extracellular membrane vesicles (EMV), ranging from nano-sized exosomes to micro-scale ectosomes, are constitutively secreted by many cell types and play a central role in intercellular communication (3-5). EMVs from CDCs contain a distinctive payload (6) and serve as agents of regeneration and cardioprotection (5,7-10); the micro-ribonucleic acids (miRNA) within these EMVs have been proposed to mediate the beneficial effects of CDCs after myocardial infarction (MI) (6).

Although EMV secretion is well characterized, the precise target cell type remains undefined. In reductionist systems, membrane vesicles are known to exert direct antiapoptotic effects on cardiomyocytes and to stimulate tube formation by endothelial cells (6,8); in contrast, little is known about EMV effects on fibroblasts, which feature prominently in scar formation and wound healing post-MI. Here we describe the beneficial effects of cardiosphere-derived EMV (CSp-EMV) and report a novel mechanism whereby EMV amplify their own bioactivity: priming dermal fibroblasts (DF) with CSp-EMV suffices to convert inert fibroblasts to therapeutically-active cells in vitro and in vivo.

METHODS

Female Wistar Kyoto rats (n = 54) 5 to 6 weeks of age were used for in vivo experiments. Human dermal fibroblasts (hDFs), human cardiospheres (hCSps) and human cardiosphere-derived extracellular vesicles (hCSp-EMV) were used for in vitro assays. To avoid any possible confounding effects of xenotransplantation, we used rat DFs (rDFs) and rat CSp-EMV (rCSp-EMV) for in vivo experiments.

To create MIs, animals underwent permanent left anterior descending (LAD) artery ligation. Four weeks later they underwent a second survival thoracotomy with animals randomly assigned to intramyocardial border zone injection utilizing 1 of 4 treatments: 1) rCSp-EMV derived from 2M cells (n = 16); 2) 2M rDFs (n = 12); 3) 2M rDFs incubated overnight with rCSp-EMV, then washed (rCSp-EMV DF, n = 16); or 4) vehicle (phosphate-buffered saline [PBS]; n = 10). The animals were monitored for an additional 4 weeks followed by endpoint functional and histological studies.

Baseline transthoracic echocardiography was performed 28 days post-MI (2 days before the second thoracotomy). Briefly, long-axis images were used to measure left ventricular end-systolic and end-diastolic volumes and ejection fraction. Short-axis M-mode images at the

level of the papillary muscle were used to measure end-systolic diameter. Follow-up echocardiographic analysis was performed 4 weeks post-injections followed by euthanasia.

CDCs were isolated from male Sprague Dawley and Brown Norway rats and cultured in Iscove's Modified Dulbecco's Medium (IMDM; Life Technologies, Carlsbad, California) supplemented with 20% fetal bovine serum (FBS) and antibiotics. To form cardiospheres, 15M CDCs were incubated with IMDM supplemented with penicillin/streptomycin and 0% FBS in ultra-low attachment dishes. Three days later, the conditioned medium was collected and processed for EMV isolation (**Figure 1A**).

An expanded Methods section is available in the **Online Appendix**.

STATISTICAL ANALYSIS

Pooled data are expressed as means ± SE. Statistical analysis was performed using factorial analysis of variance followed by a Tukey post hoc analysis of mean differences or with paired Student *t* test, indicated in figures by lines connecting compared values. A value of $p \leq 0.05$ was accepted as significant.

RESULTS

EMV CHARACTERIZATION AND INTERNALIZATION

EMVs were isolated from serum-free medium conditioned by hCSps over a period of 3 days. The final pellet contained ~12×10^9/ml of 175 ± 12 nm diameter vesicles by Nanoparticle Tracking Analysis (2) (NTA; NanoSight Ltd., Amesbury, Wiltshire, United Kingdom; **Figure 1B**). Flow cytometry revealed that these vesicles expressed tetraspanins characteristic of exosomes such as CD63, CD9, and CD81 (schematic in **Online Figure 1B** and pooled data in **Figure 1C**). Adding the final pellet to hDFs resulted in vesicle internalization as observed by confocal microscopy (**Figures 1D and 1E**). For quantification of dose-dependent vesicle internalization , images were obtained 6 **(Figures 1F, G and 1H**), 12 (**Figures 1I and 1J**), and 24 h (**Figures 1K and 1L**) after the addition of hCSp-EMV. Higher concentrations of added particles (20 to 40 × 10^9) resulted in significantly higher numbers of vesicle-laden cells, with >90% of cells positive as early as 6 h (**Figures 1G, 1I, and 1K**). Individual cells accumulate particles more rapidly at higher concentrations (**Figures 1H, 1J, and 1L**). The fluorescence per cell reached a plateau with all groups equal in intensity after 24 h of incubation (**Figure 1L**) despite persistent differences in percent uptake at steady state (**Figure 1K**). Minimal background due to free-dye internalization was observed in the cells incubated with serum containing the lipophilic dye only (**Online Figure 2**). Thus, at low vesicle concentrations, cells either take up vesicles or they do not, with comparable capacities among transduced cells. This finding provides indirect evidence against a stochastic process like membrane fusion, but is consistent with more active mechanisms of EMV uptake (endocytosis or receptor-mediated uptake).

VALIDATION OF IN VITRO BIOLOGICAL ACTIVITY OF EXTRACELLULAR MEMBRANE VESICLES

Experiments performed in vitro to assay the bioactivity of hCSp-EMV on hDFs revealed dose-dependent suppression of phosphorylated small mothers against decapentaplegic homolog (smad)2/3, smad4, and snai1, a zinc finger transcription factor and master regulator of epithelial-mesenchymal-transition (**Figures 2A through 2C**). These antifibrotic signaling changes mirror those described for CSp-conditioned media (11). To look for potential conversion of fibroblast phenotype, we evaluated the expression of fibroblast-specific protein 1 (FSP1), discoidin domain receptor 2 (DDR2), CD105, and CD90, after 24 h of hCSp-EMV incubation. Representative flow cytometry plots (**Figure 2D**) and pooled data (**Figure 2E**) reveal significant attenuation of both FSP1 and DDR2, but no effects on CD105 or CD90 expression, after single exposures to hCSp-EMV. Immunohistochemistry confirmed the reduced expression of FSP1, but also showed enhanced expression of smooth muscle actin (SMA; **Figures 2F and 2G**). The secretome of hDFs also changed after exposure to hCSp-EMV: primed hDFs secreted much higher levels of stromal-cell derived factor 1 (SDF-1) and vascular endothelial growth factor (VEGF) than unprimed hDFs (**Figures 2H and 2I**). Similar changes were seen in hDFs treated with CSp-exosomes isolated by ultracentrifugation (**Online Figure 3A**), a complementary isolation method to the default precipitation approach. Ultracentrifugation enriches EMVs and particularly exosomes, while excluding protein complexes and other debris (12). The congruence of the findings with the 2 isolation methods supports the conjecture that EMVs are primarily responsible for the biological effects investigated here. Both changes are salutary in the post-MI setting, insofar as SDF-1 promotes homing and activation of endogenous stem cells (13), while VEGF stimulates angiogenesis (1).

CARDIOPROTECTIVE AND ANGIOGENIC EFFECTS OF hCSP-EMV-PRIMED DFs

Conditioned media from hCSp-EMV-primed hDFs and hCSp-EMV per se reduced cardiomyocyte apoptosis after oxidative stress, unlike hDF-EMV (representative fluorescence activated cell sorting [FACS] plots in **Figure 3A through 3C** and pooled data in **Figure 3D**). Additionally, in an in vitro matrigel angiogenesis assay, conditioned media from hCSp-EMV-primed DFs exerted an angiogenic effect, which was as strong as that of hCSp-EMV alone; both treatments induced significantly more tube formation than hDF-EMV (representative microscope images in **Figures 3E through 3G** and pooled data in **Figure 3H**). Thus, hCSp-EMV priming confers upon hDFs the ability to stimulate angiogenesis and to protect cardiomyocytes against stress-induced apoptosis. Enhanced angiogenesis was also observed using hCSp-exosomes isolated by ultracentrifugation (**Online Figures 3B through 3D**), once again indicating that a preparation enriched in exosomes can recapitulate the beneficial effects seen with EMVs isolated by precipitation.

DISTINCTIVE microRNA PROFILES OF hCSP-EMV-PRIMED DFS

We previously reported that hCDC-derived EMVs, identified as exosomes, express a unique miRNA payload that at least partially accounts for the *in vivo* regenerative capacity of CDCs (6). Indeed, this and other reports have led to the conjecture that vesicles affect gene expression of recipient cells by miRNA transfer (14-16). To see if this mechanism might be

operating here, we first investigated the global miRNA content of hCSps and compared it to that of hDFs. A number of miRNAs were enriched in hCSps relative to hDFs: **Figure 4A** highlights those that are most abundantly overexpressed in hCSps. We then compared the miRNA profiles of CSp-EMV-primed and unprimed hDFs. **Figure 4B** reveals that hCSp-EMV-primed hDFs express very different miRNAs than unprimed hDFs (**Figure 4B**). The pattern only partially resembles that of the cells of origin (hCSps; compare to **Figure 4A**) or of the vesicles secreted by hCSps (**Figure 4C**), hinting that simple passive transfer of vesicular miRNAs cannot fully account for the distinctive miRNA profile of hCSp-EMV-primed hDFs. Finally, we compared the miRNA profiles of vesicles secreted by primed and unprimed hDFs by collecting media produced 24 h after priming by hCSp-EMV or vehicle. The miRNA profiles of primed and unprimed hDFs differed enormously (**Figure 4D**). The miRNAs secreted by hCSp-EMV-primed hDFs include several that are enriched in hCSp-EMV themselves (notably miRNA-146a, which was highlighted by Ibrahim et al. [6] and is elevated in all therapeutically-active groups here), but the patterns are otherwise quite individual. Thus, priming with hCSp-EMV leads to fundamental changes in hDF miRNA expression profiles and hDF-secreted vesicles. The distinctive miRNA profiles in hCSp-EMV-primed hDFs and their membrane vesicles argue against the possibility that the changes merely reflect accumulation and subsequent “regurgitation” of miRNAs transferred in hCSp-EMV.

rCSp-EMV-PRIMED FIBROBLASTS REVERSE REMODELING

We have presented evidence that hCSp-EMV-primed hDFs secrete SDF-1 and VEGF, exert antiapoptotic and angiogenic effects in vitro, and express distinctive miRNAs. We therefore questioned whether rCSp-EMV themselves, as well as rCSp-EMV-primed DFs, might confer therapeutic benefits in vivo in a rat model of chronic MI. One month after permanent LAD ligation, animals underwent intramyocardial injection. To assess particle biodistribution qualitatively, animals (n = 3) injected with dye-labeled rCSp-EMV were euthanized 1 h post-injection and selected organs were imaged. Approximately 20% of the injected rCSp-EMVs were found in the heart; the lungs also exhibited obvious uptake, with less in other organs (**Online Figure 4**). This percentage of retention in the heart at 1 h compares favorably with that seen with intramyocardially-injected cells (17). Minimal intensity was detected by the free dye control injections only (data not shown).

For long-term physiological experiments, animals were randomly allocated to 1 of the following 4 groups: vehicle (PBS), unprimed rDFs, rCSp-EMV, or rCSp-EMV-primed rDFs with treatment at 1 month post-MI (**Figure 5A**). One month later, echocardiography revealed improved ejection fraction in the rCSp-EMV and the rCSp-EMV-primed rDFs groups compared to either vehicle or unprimed rDFs (**Figure 5B**). This finding primarily reflected differences in left ventricular end-systolic diameter (**Figure 5C**). Histological analysis (of samples exemplified in **Figure 5D**) showed significant reductions in scar mass (**Figure 5E**) and enhanced infarct wall thickness (**Figure 5F**) in the rCSp-EMV and rCSp-EMV-primed-rDF groups. The structural and functional improvements seen with rCSp-EMV and rCSp-EMV-primed rDF were comparable to those reported with rCSp injection in this model (11).

Finally, to test the in vivo angiogenic capacity of CSp-EMV and CSp-EMV-primed cells, we quantified capillaries (bounded by von Willebrand factor-positive cells) and microvessels (bounded by SMA-positive cells; **Figure 6A**). Analysis of serial images from the apex to the base revealed greater capillary density in the rCSp-EMV and rCSp-EMV-primed groups compared to both controls in all 3 zones evaluated (infarct, border, and remote; **Figures 6B through 6D**, left panel). Microvessel density was likewise increased, but only in the infarct zone (**Figures 6B through 6D**, right panel). Another mechanism underlying CSp regenerative efficacy is cardiomyocyte proliferation (13,18). Bromodeoxyuridine incorporation revealed enhanced deoxyribonucleic acid synthesis after exposure to rCSp-EMV and rCSp-EMV-rDFs compared to PBS and unprimed rDFs, validating previous reports (6) (**Online Figures 5A and 5B**). Interestingly, this effect tended to be more prominent after rCSp-EMV-only injections compared to rCSp-EMV-rDFs. Finally, no changes in cardiomyocyte diameter were observed (**Figures 7A through 7C**).

DISCUSSION

We have observed remarkable effects of EMVs from hCSps on fibroblasts. Dermal fibroblasts are venerable controls for cardiac cell therapy; their injection neither improves nor aggravates adverse remodeling after MI (1,19). DF-produced exosomes are likewise inert (6). In contrast, cardiospheres and their progeny trigger functional recovery and structural improvements in various ischemic and nonischemic models of heart failure (20-22). This beneficial effect was recently attributed to secreted exosomes (6). Although interaction of EMVs with endothelial cells and cardiomyocytes has been reported (5,6,23,24), our data support a strong, previously unappreciated bioactivity of CSp-EMVs on fibroblasts and other cardiac cell types (**Central Illustration**). More specifically, we report that, in the restricted environment of in vitro priming with hCSp-EMV, hDFs exert a dose-dependent downregulation of the transforming growth factor (Tgf)-β cascade and increased secretion of SDF-1 and VEGF. Remarkably, these primed fibroblasts promote angiogenesis and inhibit cardiomyocyte apoptosis in vitro, while in vivo they can attenuate remodeling and improve function to levels equivalent to those reported with rCSps (11).

Vesicular transfer of miRNAs mediates cell-cell communication in different biological systems (25-27). However, the miRNA cargo of extracellular membrane vesicles does not necessarily reflect passive loading with RNAs in the parent cell; selective enrichment mechanisms appear to be at play (15). This selective miRNA payload may be a crucial determinant of bioactivity on the recipient population. Indeed, we found a distinct miRNA signature in primed versus unprimed hDFs that does not reflect passive release of internalized hCSp-EMV. Therefore, internalization of hCSp-EMV leads to downstream, biologically-significant changes in miRNA vesicular cargo released by the recipient hDFs. Additionally, since fibroblast-derived EMVs enriched in miRNAs do not improve recovery in vivo (28), the cargo transition described here may provide promising clues to pathways involved in reverse remodeling.

Many studies report the innate plasticity of fibroblasts that allows them to acquire a cardiomyocyte or endothelial phenotype after exposure to either transcription factors or small molecules (29-32). These direct reprogramming approaches may constitute a

promising therapeutic strategy (33). Our data indicate that single-dose priming with CSp-EMVs converted DFs to a less fibrotic phenotype with functional properties equal to those of CSp-EMV. Interestingly, the Tgf-β pathway, which provides key signals in cellular conversion (34,35), was significantly downregulated (**Figures 2A through 2C**). We do not yet know if EMVs or an EMV subgroup (e.g., exosomes) suffice to durably reprogram DFs to a fully-distinct cell type, but our data do indicate that inert fibroblasts can be functionally converted both in vitro and in vivo for a sufficient duration to shape therapeutic activity.

Crosstalk between endothelial cell-derived vesicles containing miRNAs and the surrounding myocardium has been reported (24). Here we demonstrated that, beyond strictly paired cell-cell communication, divergent transportation of biologically-significant signals takes place between hCSp-EMV-primed DFs and recipient human umbilical vein endothelial cells or cardiomyocytes. These findings in culture may help to rationalize the efficacy of a relatively low number of cells injected in vivo: transplanted cells secrete EMVs, which interact with the surrounding tissue and convert it into a more salutary milieu, in a positive feedback loop (2,36).

Xenogeneic transplantation of CSps post-MI elicits detrimental immunological sequelae, although allogeneic CSps are effective and immunologically innocuous (2). Here we used allogeneic rCSp-EMV to evaluate potency in vivo and allogeneic hCSp-EMV for in vitro experiments. Evaluation of the immunological sequelae of allogeneic and xenogeneic EMVs is beyond the scope of the present study, but it seems likely that CSp-EMVs may be even less immunogenic than CSps, as they express far fewer surface antigens and, unlike cells, cannot react dynamically to immunological cues.

STUDY LIMITATIONS

The cardiovascular field has previously tended to focus on exosomes, rather than EMVs as a whole (37,38). Exosomes, nano-sized particles produced by the endolysosomal pathway, are but one class of EMVs (39). The isolation method used here relies on precipitation by polyethylene glycol, which pulls down all EMVs, not just exosomes, and also macromolecules including RNA-protein complexes (39,40). Thus, it is possible that some of our results might be attributable to larger, biologically-distinct microvesicles or apoptosomes or even to non-EMV entities (e.g., free RNA or protein). Nevertheless, the size distribution (**Figure 1B**), antigenic composition (**Figure 1C**), and contents (**Figure 4**) of our default preparations are most consistent with a preponderance of exosomes (41). Key phenotypic changes are recapitulated by EMVs isolated by ultracentrifugation (**Online Figure 3**), the gold standard method for enriching exosomes (12), further implicating exosomes as mediators of the beneficial effects.

CONCLUSIONS

CSp-EMVs alter fibroblast phenotype and secretome in a salutary positive-feedback loop: exposure of “inert” fibroblasts to CSp-EMV rendered the fibroblasts therapeutic. Intramyocardially-injected CSp-EMV-primed (but not unprimed) fibroblasts increased global pump function and vessel density while reducing scar mass. The phenotypic

conversion of inert cells to therapeutically-active cells reveals a novel mechanism for amplification of exosome bioactivity.

Supplementary Material

Refer to Web version on PubMed Central for supplementary material.

Acknowledgments

FUNDING SOURCES

This work was supported by the NIH (1R01HL124074-01) and the Cedars-Sinai Board of Governors Heart Stem Cell Center.

ABBREVIATIONS

CDC	cardiosphere-derived cell
CSp-EMV	cardiosphere derived extracellular membrane vesicle
DF	dermal fibroblast
DF-EMV	dermal fibroblast-derived extracellular membrane vesicle
EMV	extracellular membrane vesicle
LAD	left anterior descending artery
MI	myocardial infarction
SDF-1	stromal-cell derived factor 1
VEGF	vascular endothelial growth factor

REFERENCES

1. Chimenti I, Smith RR, Li TS, et al. Relative roles of direct regeneration versus paracrine effects of human cardiosphere-derived cells transplanted into infarcted mice. Circ Res. 2010; 106:971–80. [PubMed: 20110532]
2. Tseliou E, Pollan S, Malliaras K, et al. Allogeneic cardiospheres safely boost cardiac function and attenuate adverse remodeling after myocardial infarction in immunologically mismatched rat strains. J Am Coll Cardiol. 2013; 61:1108–19. [PubMed: 23352785]
3. Thery C, Zitvogel L, Amigorena S. Exosomes: Composition, biogenesis and function. Nature reviews. Immunology. 2002; 2:569–79.
4. Cocucci E, Racchetti G, Meldolesi J. Shedding microvesicles: Artefacts no more. Trends Cell Biol. 2009; 19:43–51. [PubMed: 19144520]
5. Sahoo S, Klychko E, Thorne T, et al. Exosomes from human cd34(+) stem cells mediate their proangiogenic paracrine activity. Circ Res. 2011; 109:724–8. [PubMed: 21835908]
6. Ibrahim AG, Cheng K, Marban E. Exosomes as critical agents of cardiac regeneration triggered by cell therapy. Stem Cell Reports. 2014; 2:606–19. [PubMed: 24936449]
7. Heinrich EM, Dimmeler S. Micrornas and stem cells: Control of pluripotency, reprogramming, and lineage commitment. Circ Res. 2012; 110:1014–22. [PubMed: 22461365]
8. Barile L, Lionetti V, Cervio E, et al. Extracellular vesicles from human cardiac progenitor cells inhibit cardiomyocyte apoptosis and improve cardiac function after myocardial infarction. Cardiovasc Res. 2014; 103:530–41. [PubMed: 25016614]

9. Gray WD, French KM, Ghosh-Choudhary S, et al. Identification of therapeutic covariant microrna clusters in hypoxia-treated cardiac progenitor cell exosomes using systems biology. Circ Res. 2015; 116:255–63. [PubMed: 25344555]
10. Kourembanas S. Exosomes: Vehicles of intercellular signaling, biomarkers, and vectors of cell therapy. Annu Rev Physiol. 2015; 77:13–27. [PubMed: 25293529]
11. Tseliou E, Reich H, de Couto G, et al. Cardiospheres reverse adverse remodeling in chronic rat myocardial infarction: Roles of soluble endoglin and tgf-beta signaling. Basic Res Cardiol. 2014; 109:443. [PubMed: 25245471]
12. Smith JA, Ng KS, Mead BE, et al. Extracellular Vesicles. Commercial potential as byproducts of cell manufacturing for research and therapeutic use. Cell Therapies Trends and Technologies. 2015; 13(4) s. http://www.bioprocessintl.com/manufacturing/cell-therapies/extracellular-vesicles-commercial-potential-as-byproducts-of-cell-manufacturing-for-research-and-therapeutic-use/.
13. Malliaras K, Ibrahim A, Tseliou E, et al. Stimulation of endogenous cardioblasts by exogenous cell therapy after myocardial infarction. EMBO Mol Med. 2014; 6:760–77. [PubMed: 24797668]
14. Chendrimada TP, Gregory RI, Kumaraswamy E, et al. Trbp recruits the dicer complex to ago2 for microrna processing and gene silencing. Nature. 2005; 436:740–4. [PubMed: 15973356]
15. Valadi H, Ekstrom K, Bossios A, et al. Exosome-mediated transfer of mrnas and micrornas is a novel mechanism of genetic exchange between cells. Nat Cell Biol. 2007; 9:654–9. [PubMed: 17486113]
16. Alvarez-Erviti L, Seow Y, Yin H, et al. Delivery of sirna to the mouse brain by systemic injection of targeted exosomes. Nat Biotechnol. 2011; 29:341–5. [PubMed: 21423189]
17. Terrovitis JV, Smith RR, Marban E. Assessment and optimization of cell engraftment after transplantation into the heart. Circ Res. 2010; 106:479–94. [PubMed: 20167944]
18. Kuhn B, del Monte F, Hajjar RJ. Periostin induces proliferation of differentiated cardiomyocytes and promotes cardiac repair. Nat Med. 2007; 13:962–9. [PubMed: 17632525]
19. Smith RR, Barile L, Cho HC, et al. Regenerative potential of cardiosphere-derived cells expanded from percutaneous endomyocardial biopsy specimens. Circulation. 2007; 115:896–908. [PubMed: 17283259]
20. Johnston PV, Sasano T, Mills K, et al. Engraftment, differentiation, and functional benefits of autologous cardiosphere-derived cells in porcine ischemic cardiomyopathy. Circulation. 2009; 120:1075–83, 7. following 1083. [PubMed: 19738142]
21. Messina E, De Angelis L, Frati G, et al. Isolation and expansion of adult cardiac stem cells from human and murine heart. Circ Res. 2004; 95:911–21. [PubMed: 15472116]
22. Aminzadeh MA, Tseliou E, Sun B, et al. Therapeutic efficacy of cardiosphere-derived cells in a transgenic mouse model of non-ischaemic dilated cardiomyopathy. Eur Heart J. 2015; 36:751–62. [PubMed: 24866210]
23. Vrijsen KR, Sluijter JP, Schuchardt MW, et al. Cardiomyocyte progenitor cell-derived exosomes stimulate migration of endothelial cells. J Cell Mol Med. 2010; 14:1064–70. [PubMed: 20465578]
24. Hergenreider E, Heydt S, Treguer K, et al. Atheroprotective communication between endothelial cells and smooth muscle cells through mirnas. Nat Cell Biol. 2012; 14:249–56. [PubMed: 22327366]
25. Squadrito ML, Baer C, Burdet F, et al. Endogenous rnas modulate microrna sorting to exosomes and transfer to acceptor cells. Cell Rep. 2014; 8:1432–46. [PubMed: 25159140]
26. Forterre A, Jalabert A, Chikh K, et al. Myotube-derived exosomal mirnas downregulate sirtuin1 in myoblasts during muscle cell differentiation. Cell Cycle. 2014; 13:78–89. [PubMed: 24196440]
27. Siciliano V, Garzilli I, Fracassi C, et al. Mirnas confer phenotypic robustness to gene networks by suppressing biological noise. Nat Commun. 2013; 4:2364. [PubMed: 24077216]
28. Bang C, Batkai S, Dangwal S, et al. Cardiac fibroblast-derived microrna passenger strand-enriched exosomes mediate cardiomyocyte hypertrophy. J Clin Invest. 2014; 124:2136–46. [PubMed: 24743145]
29. Ubil E, Duan J, Pillai IC, et al. Mesenchymal-endothelial transition contributes to cardiac neovascularization. Nature. 2014; 514:585–90. [PubMed: 25317562]
30. Wang H, Cao N, Spencer CI, et al. Small molecules enable cardiac reprogramming of mouse fibroblasts with a single factor, oct4. Cell Rep. 2014; 6:951–60. [PubMed: 24561253]

31. Jayawardena T, Mirotsou M, Dzau VJ. Direct reprogramming of cardiac fibroblasts to cardiomyocytes using micrornas. Methods Mol Biol. 2014; 1150:263–72. [PubMed: 24744005]
32. Nam YJ, Song K, Luo X, et al. Reprogramming of human fibroblasts toward a cardiac fate. Proc Natl Acad Sci U S A. 2013; 110:5588–93. [PubMed: 23487791]
33. Marban E, Cingolani E. Direct reprogramming: bypassing stem cells for therapeutics. JAMA. 2015 [E-pub ahead of print].
34. Burridge PW, Keller G, Gold JD, et al. Production of de novo cardiomyocytes: Human pluripotent stem cell differentiation and direct reprogramming. Cell Stem Cell. 2012; 10:16–28. [PubMed: 22226352]
35. Addis RC, Epstein JA. Induced regeneration--the progress and promise of direct reprogramming for heart repair. Nat Med. 2013; 19:829–36. [PubMed: 23836233]
36. Tseliou E, de Couto G, Terrovitis J, et al. Angiogenesis, cardiomyocyte proliferation and anti-fibrotic effects underlie structural preservation post-infarction by intramyocardially-injected cardiospheres. PLoS One. 2014; 9:e88590. [PubMed: 24558402]
37. Sahoo S, Losordo DW. Exosomes and cardiac repair after myocardial infarction. Circ Res. 2014; 114:333–44. [PubMed: 24436429]
38. Hirsch E, Hilfiker-Kleiner D, Balligand JL, et al. Interaction of the heart and its close and distant neighbours: report of the Meeting of the ESC Working Groups Myocardial Function and Cellular Biology. Cardiovasc Res. 2013; 99:595–9. [PubMed: 23860811]
39. Thery C, Amigorena S, Raposo G, et al. Isolation and characterization of exosomes from cell culture supernatants and biological fluids. Curr Protoc Cell Biol. 2006; 30:3.22:3.22.1–3.22.29.
40. Van Deun J, Mestdagh P, Sormunen R, et al. The impact of disparate isolation methods for extracellular vesicles on downstream rna profiling. J Extracell Vesicles. 2014:3.
41. EL Andaloussi S, Mager I, Breakefield XO, Wood MJ. Extracellular vesicles: Biology and emerging therapeutic opportunities. Nat Rev Drug Discov. 2013; 12:347–57. [PubMed: 23584393]

PERSPECTIVES

COMPETENCY IN MEDICAL KNOWLEDGE: Cardiosphere-derived extracellular membrane vesicles (CSp-EMV) and particularly their exosomes convert inert dermal fibroblasts into therapeutically active cells capable of decreasing scar and improving function in a chronic MI model. This represents a mechanism of amplification whereby a small number of transplanted cells can exert widespread, durable benefits in injured myocardium.

TRANSLATIONAL OUTLOOK: Further animal and clinical experiments are warranted to explore the potential therapeutic roles of CSp-EMV and CSp-EMV-primed fibroblasts for diseases in which scar reduction, angiogenesis, and cardiomyocyte proliferation could be beneficial.

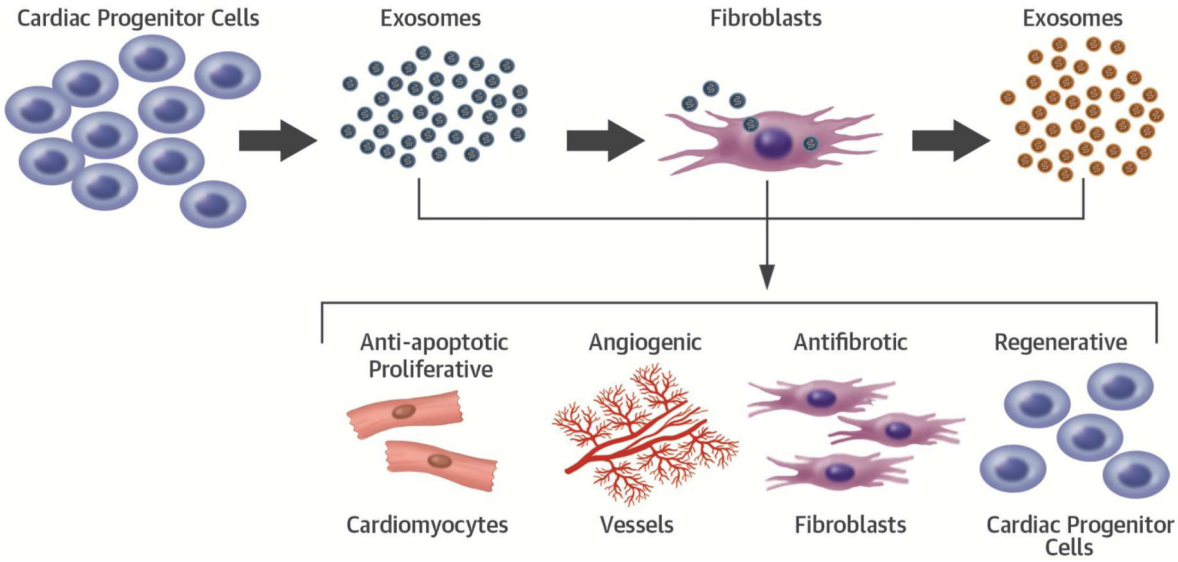

CENTRAL ILLUSTRATION. Conversion of Inert Fibroblasts to Active Cells

Cardiosphere-isolated exosomes were used to prime inert fibroblasts. Post-priming analysis of fibroblast bioactivity revealed amplification of their therapeutic properties including cardiomyogenic, angiogenic, antifibrotic, and regenerative effects.

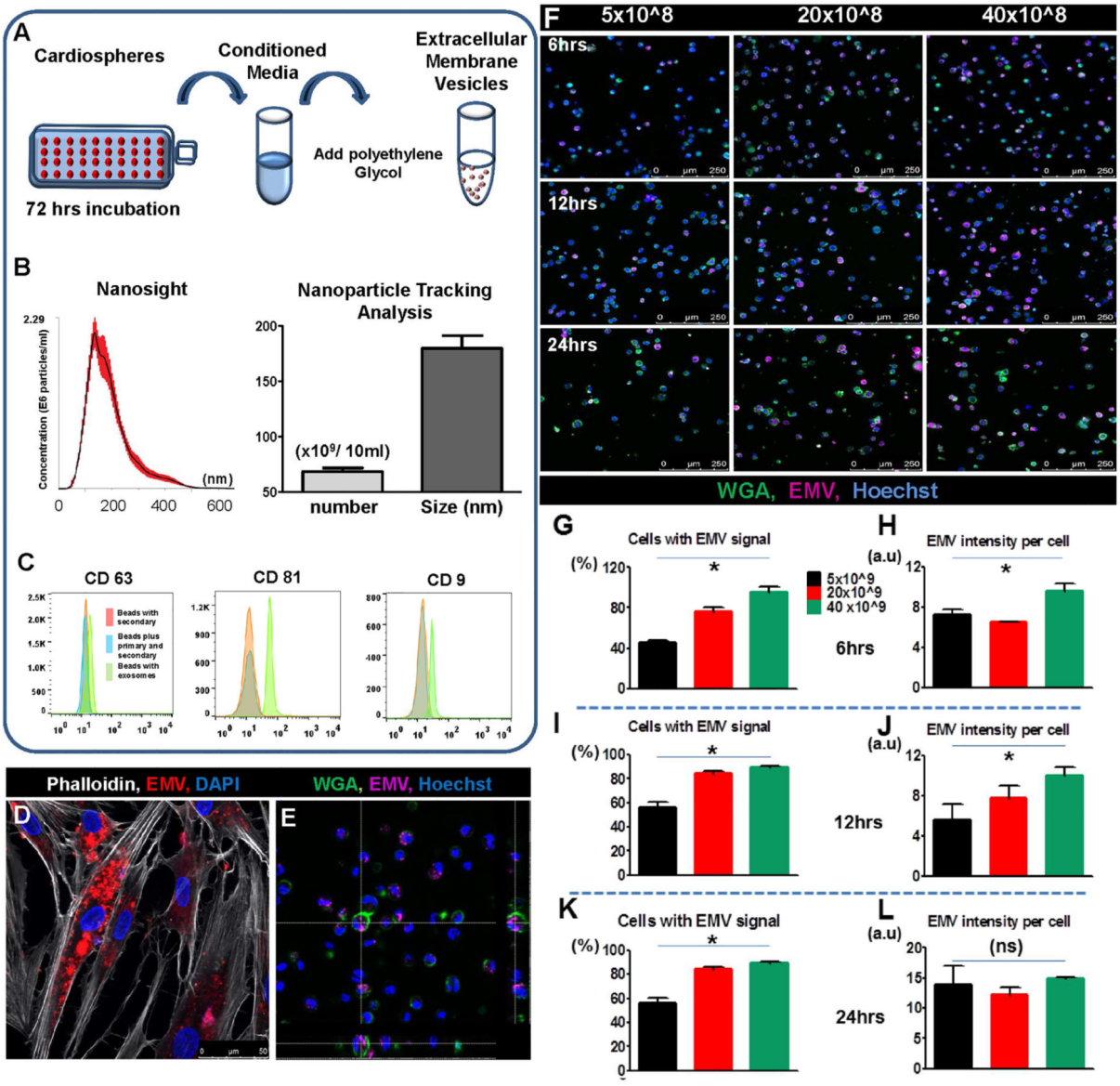

FIGURE 1. CSp-EMV Characterization and Internalization

(A) Extracellular membrane vesicles (EMV) were isolated from cardiospheres (CSp) on day 3 post-plating by adding Exoquick precipitation solution. **(B)** Size distribution was analyzed by Nanoparticle Tracking Analysis and pooled data for particle number and size quantification revealed an average size of 175 ±12 nm diameter vesicles. **(C)** Tetraspanin-bound beads were used to characterize the human CSp-derived EMVs (hCSp-EMV). Representative histograms revealed expression of CD63, CD81, and CD9. EMVs stained for tetraspanins (green line) were compared to appropriate controls (orange/blue lines). **(D)** hDFs were incubated with fluorescent dyed hCSp-EMV for 24 h followed by confocal imaging. **(E)** z-stack image of DFs 24-h post-hCSp-EMV incubation revealed particle internalization. **(F)** Representative confocal images of DFs incubated with different concentrations of hCSp-EMV and evaluation of fluorescent intensity at different time points post-incubation revealed cells with EMV signal and EMV intensity per cell at 6 h **(G and**

H), 12 h **(I and J)**, and 24 h **(K and L)** that were dose but not time dependent. Scale bar = 250 μm; n = 3-5 high-power (20×) images per group. DAPI = 4',6-diamidino-2-phenylindole; DF = dermal fibroblast; WGA = wheat germ agglutinin.

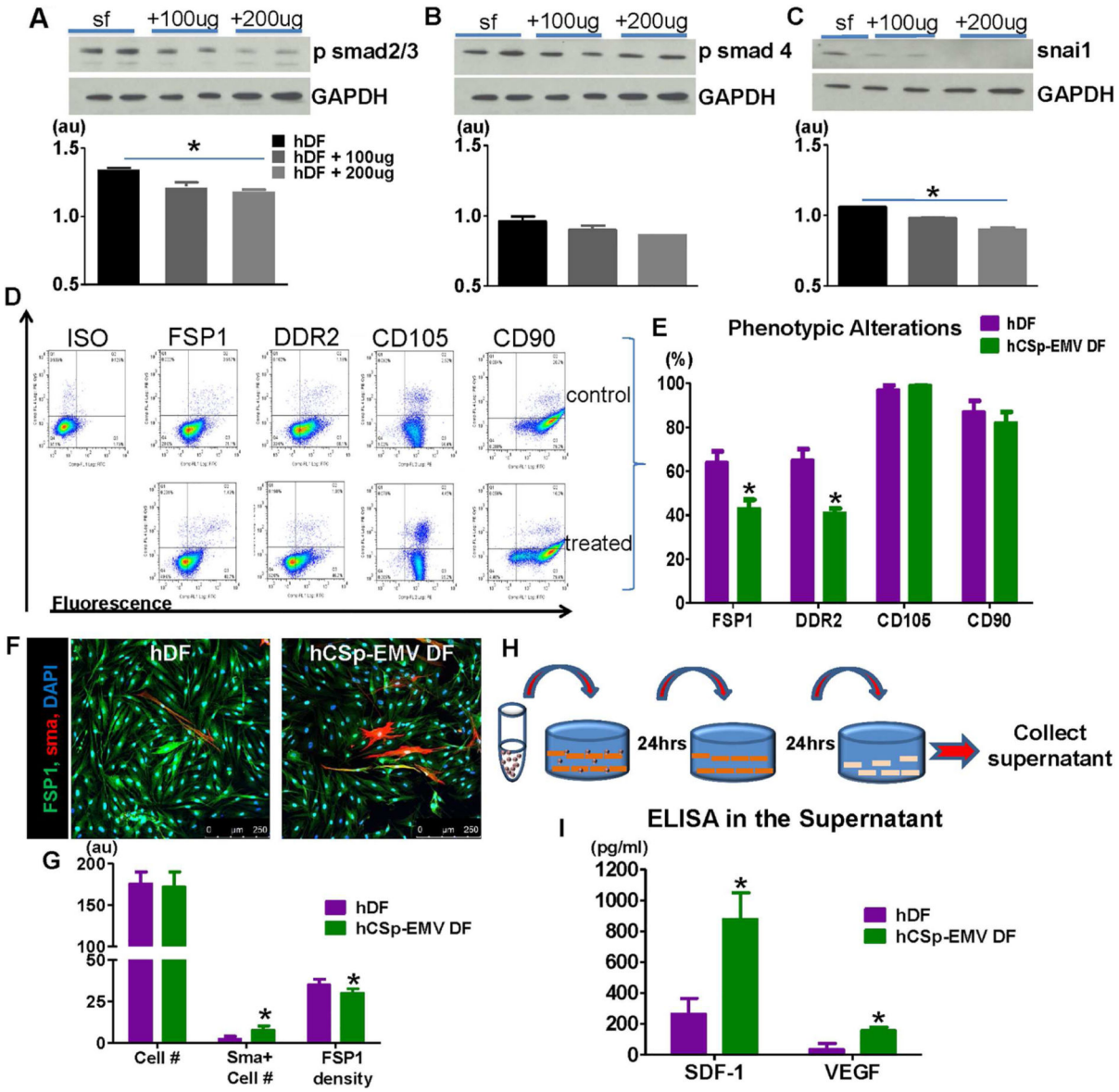

FIGURE 2. In Vitro Characterization of CSp-EMV Biological Activity

Western blot of hDFs 24 h post-incubation with 2 different concentrations of hCSp-EMV showed reduced psmad2/3 **(A)**, psmad4 **(B)**, and snai1 **(C)**. Glyceraldehyde 3-phosphate dehydrogenase (GAPDH) was used as a control. The experiment was performed in triplicates. Flow cytometry was used for phenotypic characterization of the hCSp–EMV-primed fibroblasts 24 h post-incubation. Representative FACS plots **(D)** and pooled data **(E)** revealed reduced fibroblast-specific protein 1 (FSP1) and discoidin domain receptor 2 (DDR2) expression while CD105 and CD90 were not affected (n = 3 in each group). Confocal images of hCSp-EMV-primed and -unprimed fibroblasts **(F)** showed enhanced density of the smooth muscle actin (SMA) cells and lower FSP1 density post-CSp-EMV incubation **(G)**. Scale bar = 250 µm. **(H)** Scheme of the collected supernatant post hCSp-EMV treated fibroblasts; **(I)** enzyme-linked immunosorbent assay (ELISA) on the collected supernatant revealed increased levels of SDF-1 and VEGF in the post primed fibroblasts. n =

5 per group. *p < 0.05 vs. unprimed fibroblasts. FACS = fluorescence activated cell sorting; ISO = isotype control; smad = small mothers against decapentaplegic homolog; other abbreviations as in Figure 1.

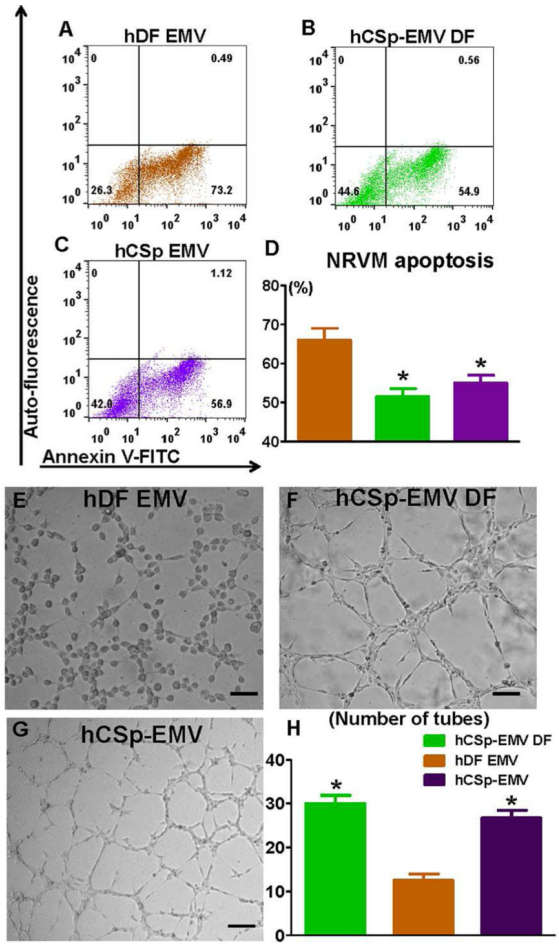

FIGURE 3. In Vitro Bioactivity of CSp-EMV-primed Fibroblasts

Representative FACS plots of neonatal rat ventricular myocytes (NRVM) were treated with **(A)** hDF-EMVs, **(B)** conditioned media from hCSp-EMV-primed hDFs, and **(C)** hCSp-EMVs for 72 h and stained with Annexin V to evaluate apoptosis. The experiment was performed in triplicates (n = 3 for each group). **(D)** Pooled data for the NRVM apoptosis revealed higher viability in the hCSp-EMV-primed fibroblast and hCSp-EMV groups compared to the DF-EMVs. (Histogram color = group in bar graph.) **E-G.** Representative higher power images of the Matrigel tube formation assay from **(E)** hDF-EMVs, **(F)** conditioned media from hCSp-EMV-primed hDFs, and **(G)** hCSp-EMVs and **(H)** pooled data for tube quantification. Similarly, enhanced tube formation was observed in the latter 2 groups compared to the hDF-EMV only. *$p < 0.05$ vs. DF. Scale bar = 50 μm. Abbreviations as in Figures 1 and 2.

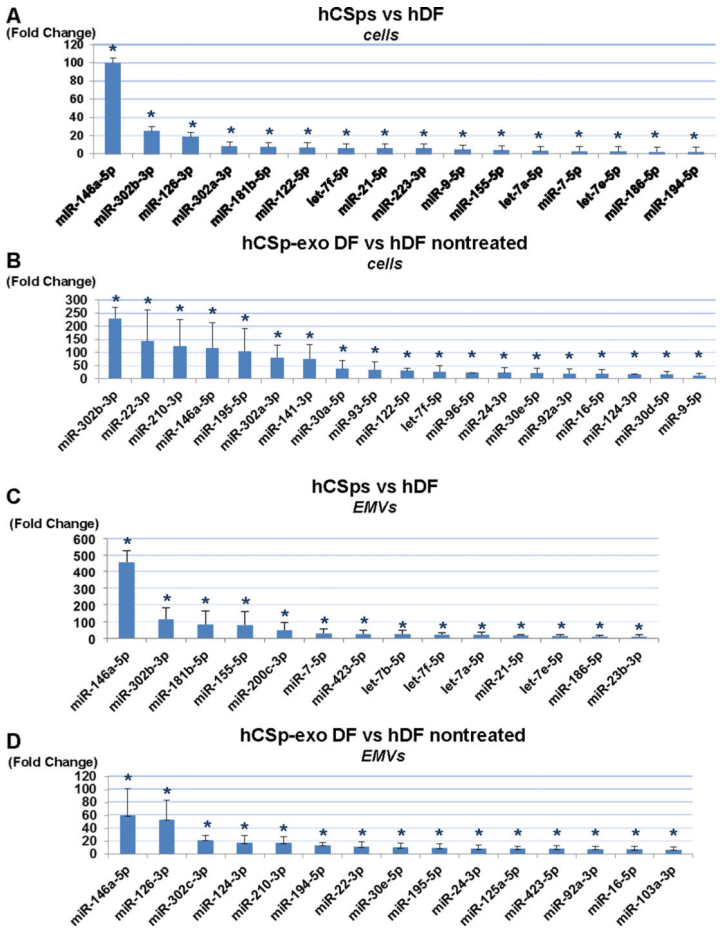

FIGURE 4. MiRNA Array Analysis: Signature of Secreted Extracellular Vesicles and Parent Cells

Micro-ribonucleic acid (miRNA) with statistically significant fold changes are seen in **(A)** hCSps versus hDFs and **(B)** hCSp-EMV-primed DFs versus unprimed hDFs. Additionally, fold ratios of miRNA profiles from EMVs derived either from hCSps or unprimed hDFs **(C)** and fold changes in the miRNA cargo of the EMVs secreted by hCSp-EMV-primed hDFs versus unprimed hDFs **(D)** are seen. All $p<0.05$. $n = 3$ per group. Abbreviations as in Figure 1.

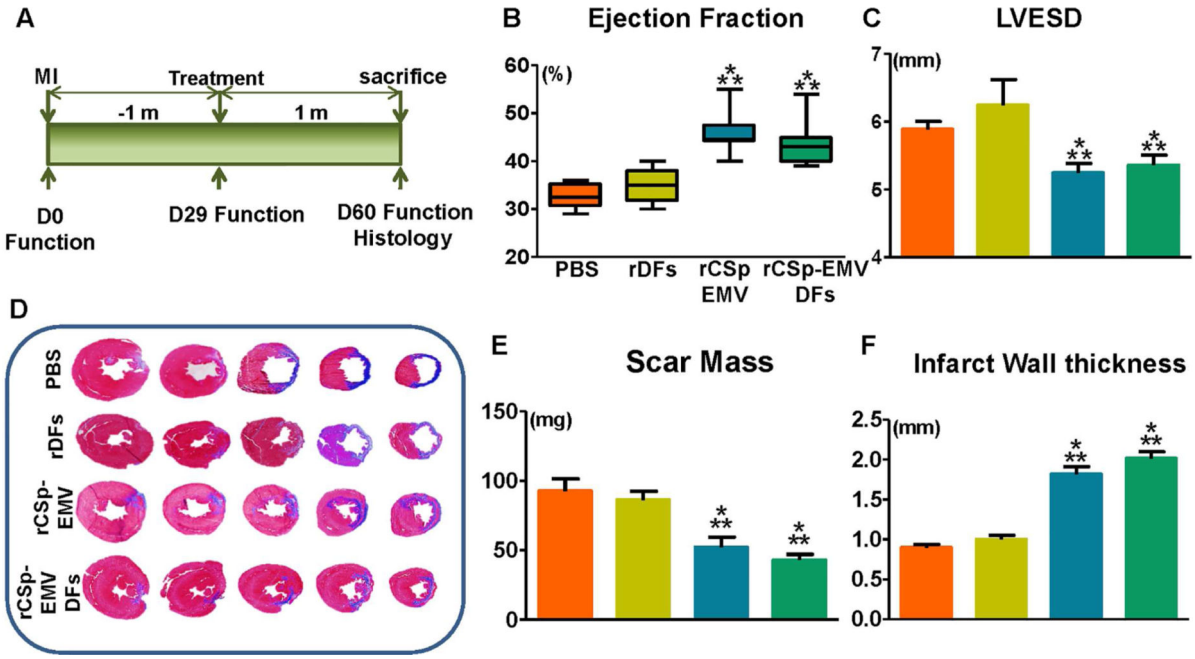

FIGURE 5. In Vivo Studies

According to the study timeline **(A)**, myocardial infarction was induced in Wistar Kyoto rats; 1 month later, the animals were allocated to injection of vehicle (PBS; orange bars; n = 6), rDFs (yellow; n = 8), rDFs primed with rCSp-EMV (green; n = 8), or rCSp-EMV only (blue; n = 8). Functional follow-up and histological analysis were performed 1 month post-injection. At 1 month post-injection, rCSp-EMV and rCSp-EMV-primed rDFs demonstrated significant improvement in cardiac function via ejection fraction **(B)** as well as better-maintained left ventricular end-systolic diameter (LVESD) via M-mode short axis images **(C)** compared to control groups. Scar mass was evaluated by serial Masson's Trichrome stained sections from the left ventricle **(D)**, and was significantly reduced in the rCSp-EMV and the rCSp-EMV-primed rDF groups compared to either control group **(E)**.Significant differences also were observed in infarct wall thickness **(F)**. *p<0.05 vs. DFs; **p < 0.05 vs. PBS. PBS = phosphate-buffered saline; rCSp = rat cardiosphere; rDFs = rat dermal fibroblasts; other abbreviations as in Figure 1.

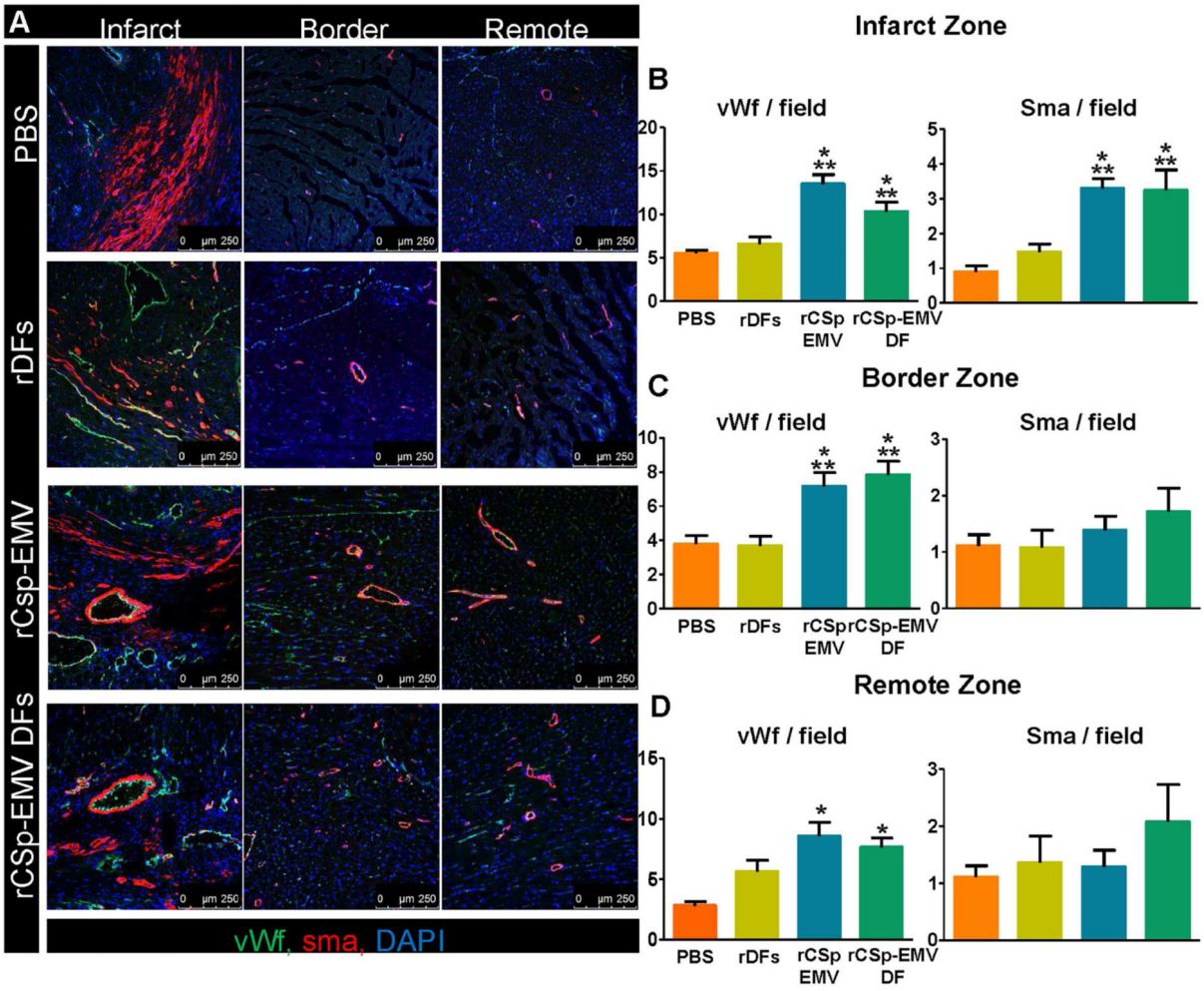

FIGURE 6. In Vivo Vessel Density 1-month Post-treatment

(A) Representative immunostained images from the infarct, border, and remote zones are presented for evaluation of microvessel and capillary density. In the infarct **(B)**, border **(C)**, and remote **(D)** zones, pooled data revealed enhanced von Willebrand factor (vWf)-positive capillary density in the rCSp-EMV and rCSp-EMV-primed rDF groups compared to both controls (left panels) and changes regarding SMA-positive vessels (right panels). n = 5 in each of the groups. Scale bar = 250 μm. *p < 0.05 vs. DFs; **p < 0.05 vs. PBS. Abbreviations as in Figures 1, 2, and 5.

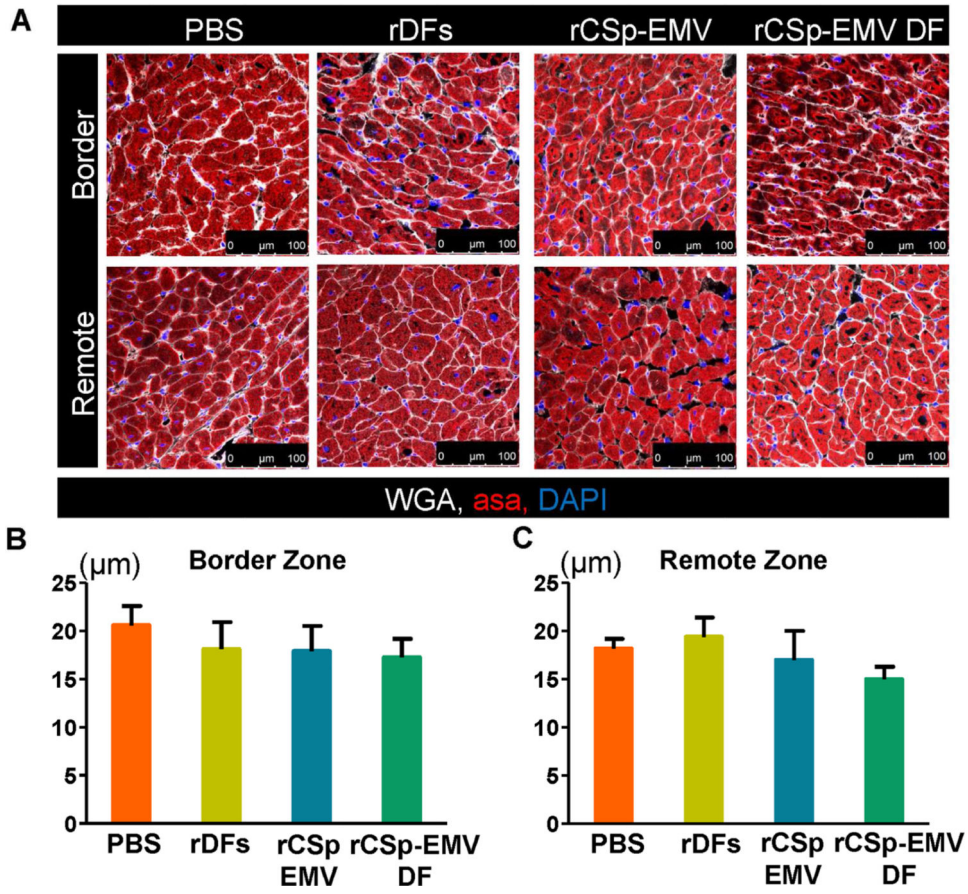

FIGURE 7. In Vivo Cardiomyocyte Architecture 1-month Post-therapy

(A) Representative immunostained images from the border and remote zones were used for evaluation of cardiomyocyte diameter. Pooled data revealed no difference between the groups analyzed in the border **(B)** and remote **(C)** zones. n = 5 in each of the groups. Scale bar = 100 μm. ASA =α- sarcomeric actin; other abbreviations as in Figures 1 and 5.